Published in final edited form as:

Inorg Chem. 2011 February 21; 50(4): 1570–1579. doi:10.1021/ic102300d.

Chemistry of Nitrosyl Iron Complexes Supported by a β-Diketiminate Ligand

Zachary J. Tonzetich, **Florent Héroguel**, **Loi H. Do**, and **Stephen J. Lippard***

Department of Chemistry, Massachusetts Institute of Technology, Cambridge, MA 02139

Abstract

Several nitrosyl complexes of Fe and Co have been prepared using the sterically hindered Ar-nacnac ligand (Ar-nacnac = anion of [(2,6-diisopropylphenyl)NC(Me)]$_2$CH). The dinitrosyl iron complexes, [Fe(NO)$_2$(Ar-nacnac)] (**1**) and (Bu$_4$N)[Fe(NO)$_2$(Ar-nacnac)] (**2**) react with [Fe^{III}(TPP)Cl] (TPP = tetraphenylporphine dianion) to generate [Fe^{II}(TPP)(NO)] and the corresponding mononitrosyl iron complexes. The factors governing NO-transfer with DNICs **1** and **2** are evaluated, together with the chemistry of the related mononitrosyl iron complex, [Fe(NO)Br(Ar-nacnac)], **4**. The synthesis and properties of the related cobalt dinitrosyl [Co(NO)$_2$(Ar-nacnac)], **3**, is also discussed for comparison to DNICs **1** and **2**. The solid-state structures of several of these compounds as determined by X-ray crystallography are reported.

INTRODUCTION

The potential for dinitrosyl iron complexes (DNICs) to serve as storage and transfer units for nitric oxide in vivo has stimulated interest in biomimetic chemistry that reveals the principles underlying such reactivity.[1] Much of this interest stems from the demonstration that DNICs can participate in a host of physiological processes normally mediated by NO gas.[2-8] DNICs also hold promise as therapeutic delivery agents of NO.[9-14] The release of free NO by iron nitrosyls has been examined in detail, yet very little work has been devoted to understanding the mechanism of NO-transfer from DNICs.[15-18] In a biological context, the transfer of NO can be tedious to study since the nature of a DNIC can be difficult to ascertain. Broadly defined, dinitrosyl iron complexes are any member of a class of compounds containing the {Fe(NO)$_2$} unit,[19] although the moniker DNIC is typically reserved for thiolate-bound, mononuclear complexes of the type [Fe(NO)$_2$(SR)$_2$]$^-$.[20,21] Biologically, the $^-$SR anion typically derives from cysteinate residues in proteins or mobile units such as glutathione, although examples of biological DNICs with non-thiolate ligands are also known.[22,23]

Formation of DNICs in vivo occurs through interaction of NO with chelatable pools of ferrous iron[24] or by attack of NO on protein-based iron centers such as iron-sulfur clusters.[25-31] Mononuclear DNICs that result are denoted {Fe(NO)$_2$}^{9} in the Enemark-Feltham

*lippard@mit.edu.

Supporting Information Available. Additional figures, complete spectra, crystallographic data, and fully labeled thermal ellipsoid diagrams for compounds **3** – **6**, as well as the corresponding CIF files. This information is available free of charge via the Internet at http://pubs.acs.org.

notation[32] and display a characteristic g_{avg} = 2.03 EPR signal arising from an S = ½ groundstate.[33] The precise electronic structure of $\{Fe(NO)_2\}^9$ DNICs remains a point of contention, and descriptions ranging from {HS-Fe(I)}–$\{^2(NO\cdot)\}_2$, to {HS-Fe(III)}-$\{^3(NO^-)\}_2$, to {Fe(-I)}–$\{^1(NO^+)\}_2$, where HS denotes "high-spin," have been proffered.[34–39] A more detailed knowledge of DNIC electronic structure is important for understanding both the nature of the metal-nitrosyl bond and the mechanism of NO transfer. Such information would also facilitate comparison with the chemistry of nitrosothiols, which are generally agreed to play an important role in NO-mediated processes.[40,41]

Implicit to a discussion of NO-transfer reactivity is the question of NO redox state. Three different scenarios are possible for transfer of the nitrosyl group from donor to acceptor, formally involving NO^+, NO·, and NO^- and resulting in oxidative nitrosylation (nitrosation), nitrosylation, or reductive nitrosylation of the acceptor moiety, respectively (Scheme 1). With nitrosothiols, reductive nitrosylation is unlikely because the reaction would require formation of RS^+. With metal-nitrosyls, however, transfer of each redox form of NO must be considered. An added layer of complexity to the chemistry of DNICs is their ability to participate in redox chemistry prior to NO transfer. DNICs containing the $\{Fe(NO)_2\}^9$ unit display an electrochemically reversible one-electron reduction to the diamagnetic $\{Fe(NO)_2\}^{10}$ state. With π-acidic ligands such as carbonyls, phosphines, and certain nitrogen-based ligands, such reduced species have been isolated and characterized.[42] With thiolate (RS^-) ligands, however, chemical reduction of the $\{Fe(NO)_2\}^9$ DNIC leads to dissociation of disulfide (RSSR) and dimerization to form a valence delocalized $\{Fe(NO)_2\}^9$-$\{Fe(NO)_2\}^{10}$ species.[43,44]

Recently, we reported the synthesis of a pair of homologous DNIC redox partners, $\{Fe(NO)_2\}^{9/10}$, containing a sterically hindered β-diketiminate ligand (Chart 1, compounds **1** and **2**).[45] The identical ligand sets in these DNICs permit an evaluation of the effect that iron redox state plays on their structures and reactivity. One very interesting observation from this study is that the isomer shifts (δ) in the Mössbauer spectra of the two DNICs are nearly identical, δ 0.19(2) and 0.23(2) mm/s for **1** and **2**, respectively, which is unexpected for a metal-centered reduction.[34] This result clearly reveals the intricate nature of the electronic structure of $\{Fe(NO)_2\}$ units and indicates that redox reactions of DNICs are more complex than anticipated from simple metal-based processes.

In the present work we have used these well-defined dinitrosyl iron complexes to investigate the mechanism of NO-transfer. The β-diketiminate ligand, Ar-nacnac (Ar = 2,6-diisopropylphenyl),[46,47] is critical to this study because it helps stabilize both the DNIC starting materials and the products of NO-transfer. Moreover, the nitrogen-rich coordination environment afforded by the Ar-nancac ligand is a reasonable approximation of the histidine residue N-donor atoms.[48,49]

RESULTS

Dinitrosyl Complexes

The synthesis and characterization of DNICs **1** and **2** were described previously.[45] Each compound has pseudo-tetrahedral coordination geometry with the $\{Fe(NO)_2\}$ unit residing

in a pocket created by the sterically demanding diisopropylphenyl substituents. Compounds **1** and **2** are thermally robust and display sharp melting points at temperatures above 150 °C. Compound **1** is stable in air for short periods of time whereas compound **2** oxidizes rapidly in the presence of dioxygen to generate **1** (Figure S1). Both compounds display an electrochemically reversible one-electron couple at −1.34 V vs Fc/Fc^+ in tetrahydrofuran (Figure S2). This potential is higher than that observed for DNICs containing thiolate ligands, reflecting the neutral character of **1**. Other examples of neutral DNICs with mixed histidine/thiolate ligands have comparable potentials for the $\{Fe(NO)_2\}^{9/10}$ couple.[50]

As a means of comparison to compounds **1** and **2**, the cobalt analog, $[Co(NO)_2(Ar\text{-}nacnac)]$, was prepared. A variety of $\{Co(NO)_2\}^{10}$ species have been reported previously, and these compounds are generally similar to the corresponding $\{Fe(NO)_2\}^9$ species.[51,52] The dicobalt precursor, $[Co(NO)_2(\mu\text{-}Cl)]_2$,[53] was chosen as a starting material for the synthesis of $[Co(NO)_2(Ar\text{-}nacnac)]$. Reaction of Na(Ar-nacnac) with $[Co(NO)_2(\mu\text{-}Cl)]_2$ in tetrahydrofuran or diethyl ether afforded the desired $\{Co(NO)_2\}^{10}$ species, **3**, in moderate yield after recrystallization from pentane. The compound is diamagnetic as expected for a $\{M(NO)_2\}^{10}$ species, giving a sharp, well-resolved ^1H NMR spectrum at 25 °C in benzene-d_6. Much like compounds **1** and **2**, compound **3** displays two intense IR peaks arising from the two nitrosyl ligands. These peaks appear at 1801 and 1706 cm^{-1} in benzene-d_6 and should be compared with values of 1761 and 1709 cm^{-1} and 1627 and 1567 cm^{-1} for **1** and **2**, respectively. The solid-state structure of **3** is displayed in Figure 1 (see Table 1 for refinement details). Compound **3** crystallizes with two chemically equivalent but crystallographically independent molecules in the asymmetric unit. Like **1** and **2**, compound **3** displays pseudo-tetrahedral geometry at the metal center with the flanking diisopropylphenyl groups creating a pocket for the $\{Co(NO)_2\}^{10}$ unit. The geometric parameters about the nitrosyl ligands compare well with those in **1** and **2** but have slightly shorter N–O bond lengths (avg. of 1.15 Å) consistent with the poorer π-backbonding ability of Co(I) versus Fe(I) and Fe(0).

Compound **3** was examined by cyclic voltammetry to determine whether the $\{Co(NO)_2\}^9$ state could be accessed electrochemically. The CV displayed no reversible oxidation in tetrahydrofuran, but did exhibit a quasi-reversible cathodic process at −1.80 V (Figure 2). Reduction of the $\{Co(NO)_2\}^{10}$ core is surprising considering that a putative $\{Co(NO)_2\}^{11}$ species would have 19 electrons. Chemical reduction of **3** was attempted with KC_8 in benzene. IR, UV-vis, and EPR spectra of the resulting reduced species are all consistent with a $\{Co(NO)_2\}^{11}$ complex (see SI). A new optical band appeared at 607 nm upon reduction. Addition of dry air to this reduced species resulted in disappearance of the band at 607 nm and regeneration of **3**, as judged by UV-vis spectroscopy (Figure S5). The IR bands of **3** disappear upon reduction, being replaced with lower energy bands < 1600 cm^{-1}. Unfortunately, the $\{Co(NO)_2\}^{11}$ complex could not be isolated. The K^+ ions appear to be important in stabilizing the reduced species, because attempts to replace them by treatment with Bu_4NCl and PPNCl (PPN = cation of μ-nitridobis(triphenylphosphine)) failed, resulting in decomposition.

Mononitrosyl Complexes

The success of the β-diketiminate in stabilizing compounds containing both $\{Fe(NO)_2\}^9$ and $\{Fe(NO)_2\}^{10}$ units prompted us to evaluate its potential as a ligand for the $\{Fe\text{-}NO\}^7$ unit. Furthermore, mononitrosyl iron complexes (MNICs) are relevant to NO-transfer chemistry because they represent logical byproducts of nitrosyl loss from DNICs. The synthesis of a compound containing the $\{Fe\text{-}NO\}^7$ unit was accomplished by salt metathesis of the lithium or sodium diketiminate with the mononitrosyl precursor, (M)[Fe(NO)Br_3] (eq 1, M = Et_4N or PPN). Upon addition of the diketiminate salt to [Fe(NO)Br_3]$^-$, an immediate color change from yellow-brown to dark green occurred, indicating formation on a new species. The precise nature of this initial complex is unknown, but most likely corresponds to a dibromo complex having the formula (M)[Fe(NO)Br_2(Ar-nacnac)] (***4′***). After several hours at 25 °C, Et_4NCl or PPNCl precipitated and the supernatant changed from green to dark brown, indicating formation of the desired compound, [Fe(NO)Br(Ar-nacnac)] (**4**). Prolonged reaction times were detrimental to both the yield and purity of **4** due to competing disproportionation to form **1** (vide infra).

$$(M)\,[Fe(NO)_3Br] + Na\,(Ar-nacnac) \rightarrow \underset{4,\{Fe-NO\}^7}{[Fe\,(NO)\,Br\,(Ar-nacnac)]} + MBr + NaBr \quad (1)$$

MNIC **4** is a dark brown crystalline solid that is soluble in common organic solvents including alkanes. Its IR spectrum displays an intense peak at 1777 cm^{-1} (benzene-d_6) corresponding to the ν_{NO} fundamental (see SI). Substitution with ^{15}NO leads to a 34 cm^{-1} red-shift, consistent with a simple harmonic oscillator (calculated $\Delta\nu_{NO}$ = 32 cm^{-1}). As with other mononuclear $\{Fe\text{-}NO\}^7$ species, **4** is paramagnetic. Its EPR spectrum at 77 K in a 2-MeTHF glass is consistent with an S = $^3/_2$ ground state (see SI). Such a spin-state for a four-coordinate $\{Fe\text{-}NO\}^7$ species is not uncommon and has been observed for both [Fe(NO)Br_3]$^-$ and [Fe(NO)(S-*t*-Bu)$_3$]$^-$.[54,55]

The solid-state structure of **4** is displayed in Figure 3 (see Table 1 for refinement details). Much like compounds **1** and **2**, compound **4** is pseudo-tetrahedral with an acute bite angle for the Ar-nacnac ligand. The Br and NO groups are disordered in the crystal lattice, but were modeled satisfactorily with occupancies of 67% and 33% for the major and minor components, respectively. In addition, the thermal ellipsoid for the oxygen atom of the NO group is elongated in a plane perpendicular to the N–O bond vector. This elongation may be a consequence of slight non-linearity of the Fe–N–O bond angle that could not be effectively modeled due to the proximity of the disordered bromine atom. The geometric parameters about the iron nitrosyl unit (see Figure 3 caption) are similar to those reported for other $\{Fe\text{-}NO\}^7$ species.[54,56] The Mössbauer spectrum of **4** (see SI) displays a single quadrupole doublet with an isomer shift of 0.33(2) mm/s and a quadrupole splitting of 0.92(2) mm/s. The isomer shift compares moderately well with that of 0.26(2) mm/s reported for [Fe(NO)(S-*t*-Bu)$_3$]$^-$,[54] but is substantially lower than values for 5- and 6-coordinate S = $^3/_2$ $\{Fe\text{-}NO\}^7$ species, which typically fall between 0.62 and 0.77 mm/s.[57]

The cyclic voltammogram of **4** in tetrahydrofuran displays a quasi-reversible one-electron reduction at −1.23 V (vs Fc/Fc^+) corresponding to the $\{Fe\text{-}NO\}^{7/8}$ couple. Upon cycling of

this couple at 100 mV/s, a new species formed having a midpoint potential of −1.34 V (Figure 4). This value corresponds to the $\{Fe(NO)_2\}^{9/10}$ couple previously observed for compounds **1** and **2**, suggesting that the $\{Fe\text{-}NO\}^8$ species is unstable with respect to transformation to a dinitrosyl iron complex.

The electrochemical results with **4** were corroborated chemically using Cp^*_2Co (Cp^* = pentamethylcyclopentadiene) as a reductant. Upon addition of Cp^*_2Co to solutions of **4** in benzene-d_6, an immediate change in color from dark brown to yellow-brown was observed. NMR and IR spectra of the reaction mixtures confirmed the presence of **2** along with a new paramagnetic Fe species. Simple stoichiometry requires the formation of a new Fe(II) species, as indicated in eq 2.

$$\underset{\{Fe-NO\}^8}{[Fe(NO)Br(Ar-nacnac)]^-} \rightarrow 1/2\underset{2,\{Fe(NO)_2\}^{10}}{[Fe(NO)_2(Ar-nacnac)]^-} + 1/2\left[Fe^{III}Br_2(Ar-nacnac)\right]^- \quad (2)$$

An Fe(II) bromide complex could be prepared independently by reaction of the sodium salt of the β-diketiminate ligand with anhydrous $FeBr_2$ in THF. This new compound, **5**, was isolated as a yellow THF adduct after crystallization from THF/pentane (Figure 5). Divalent iron halide species similar to **5** have been prepared previously as dimers in the absence of a coordinating solvent.[58] The ^{1}H NMR features of **5** are nearly identical to those observed for the Fe(II) species formed by reduction of **4** suggesting that **5**, or a related complex such as the dibromide anion shown in eq 2, is generated concomitant with **2** during disproportionation of the putatative $\{Fe\text{-}NO\}^8$ species. Compound **5** loses THF in vacuo to form an orange species, which is most likely the dimeric $[Fe_2(\mu\text{-}Br)_2(Ar\text{-}nacnac)_2]$ (**5′**). Dimeric **5′** has poor solubility in non-coordinating solvents, but dissolves readily in THF to regenerate **5**. Compound **5** also serves as a convenient synthon for MNIC **4**, which forms by simple addition of NO gas (eq 3). In this manner, the ^{15}N-analog of **4** can be prepared directly from ^{15}NO (g).

$$\underset{5}{\left[Fe^{II}(THF)Br(Ar-nacnac)\right]} + NO(g) \rightarrow \underset{4,\{Fe-NO\}^7}{[Fe(NO)Br(Ar-nacnac)]} + THF \quad (3)$$

Disproportionation of the $\{Fe\text{-}NO\}^8$ unit accounts for the observation that samples of recrystallized **4** contain small amounts of **1**, since the $\{Fe\text{-}NO\}^7$ complex may be reasonably supposed to disproportionate to **1** and an Fe(III) species in an analogous fashion to its reduced counterpart, albeit at a much slower rate. To test this hypothesis, the Fe(III) complex $[FeBr_2(Ar\text{-}nacnac)]$ (**6**) was prepared.[59] Isolation and purification of $[Fe^{III}Br_2(Ar\text{-}nacnac)]$ was complicated by competing reduction of Fe(III) by the Ar-nacnac ligand.[60] Nevertheless, small quantities of **6** could be isolated, and the solid-state structure is displayed in Figure 6 (see also Table 1). Upon mixing solutions of compounds **1** and **6** at ambient temperature, partial conversion to MNIC **4** was observed by IR spectroscopy over 24 h. This observation suggests that all three species, **1**, **4**, and **6**, can interconvert (eq 4), with the equilibrium lying predominantly toward **4**. Upon reduction, a similar situation

exists involving compounds **2**, **5**, and the {Fe-NO}^{8} complex, but in this instance the equilibrium lies entirely toward **2** and **5** (eq 2).

$$\underset{1,\{Fe(NO)_2\}^9}{[Fe(NO)_2\,(Ar-nacnac)]}+\underset{6}{\left[Fe^{III}Br_2\,(Ar-nacnac)\right]} \rightleftarrows 2\,\underset{4,\{Fe-No\}^7}{[Fe\,(NO)\,Br\,(Ar-nacnac)]} \quad (4)$$

NO Transfer Reactions

NO-transfer experiments were undertaken with DNICs **1** and **2** using [Fe^{III}(TPP)Cl] (TPP = *meso*-tetraphenylporphine) as the NO acceptor. This porphyrin complex was chosen because of the documented importance of Fe heme compounds to the biological chemistry of NO and the precedent for transfer of NO from DNICs to Fe porphyrins.[16,17,61] Furthermore, porphyrin compounds have intense optical bands that facilitate reaction monitoring by UV-vis spectroscopy. Addition of **1** to THF or benzene solutions of [Fe^{III}(TPP)Cl] resulted in little to no reaction at 25 °C over several hours in the absence of light. Upon heating (50 to 80 °C) and/or irradiation with room light, however, a new Fe(TPP) species formed within one hour. When the reaction was followed by optical spectroscopy, a clean conversion to the new Fe porphyrin species was detected, with several isosbestic points indicating an A → B type process (Figure 7). UV-vis and IR spectral studies confirmed the identity of the new species as the nitrosylated {Fe-NO}^{7} porphyrin, [Fe^{II}(NO)(TPP)].[62] IR spectroscopy also identified a new NO-containing compound with a ν_{NO} stretch near 1770 cm^{-1}. This value agrees well with that found for compound **4** (vida supra) and most likely corresponds to the related mononitrosyl iron complex, [Fe(NO)Cl(Ar-nacnac)]. These results indicate that NO-transfer from **1** to [Fe^{III}(TPP)Cl] formally involves transfer of NO$^-$ with reductive nitrosylation of the ferric porphyrin. Upon transfer of NO$^-$ from DNIC **1** the corresponding {Fe-NO}^{7} MNIC is generated, a process that can be described by the stoichiometry displayed in eq 5.

$$\underset{1,\{Fe(NO)_2\}^9}{[Fe(NO)_2\,(Ar-nacnac)]}+\left[Fe^{III}Cl\,(TPP)\right] \rightarrow \underset{\{Fe-NO\}^7}{[Fe\,(NO)\,Cl\,(Ar-nacnac)]}+\underset{\{Fe-NO\}^7}{\left[Fe^{II}\,(NO)\,(TPP)\right]} \quad (5)$$

Initial kinetic studies of the reaction employing excess **1** at several temperatures > 50 °C displayed complex behavior that could not be fit to a pseudo first-order process (e.g., Figure 8). Although inconclusive, the data suggest that NO transfer from **1** is unimolecular in DNIC concentration and independent of [Fe^{III}(TPP)Cl]. For example, halving the DNIC concentration led to an ~50% decrease in reaction rate, whereas halving the [Fe^{III}(TPP)Cl] concentration led to no discernable change. These observations are consistent with a mechanism that involves rate-limiting dissociation of NO· or NO$^-$ from **1** followed by rapid capture of the nitrosyl (or nitroxyl) fragment by [Fe^{III}(TPP)Cl] and immediate transfer of Cl· or Cl$^-$ to the resulting {Fe-NO}^{8} or {Fe-NO}^{7} species, respectively. Other mechanistic scenarios involving subsequent fast electron transfer steps are also consistent with the data. Based on the observed decomposition route of the {Fe-NO}^{8} species, however, we favor a pathway involving direct formation of {Fe-NO}^{7} from **1**.

In order to compare the effect of DNIC redox state on NO-transfer reactivity, the reaction of **2** with [Fe^{III}(TPP)Cl] was also examined. As with DNIC **1**, reaction of the ferric porphyrin with DNIC **2** cleanly afforded [Fe^{II}(NO)(TPP)]. In contrast to reactions with **1**, however, NO-transfer with **2** proceeded in the absence of light and/or heat over the course of 4 h in benzene-d_6. Compound **2** is consumed immediately upon reaction with [Fe^{III}(TPP)Cl] as judged by IR spectroscopy (Figure 9). UV-vis spectroscopy confirmed that reduction of [Fe^{III}(TPP)Cl] takes place prior to NO transfer to generate **1** (Figure 8: 1761, 1708 cm^{-1}) and the ferrous porphyrin [Fe^{II}(TPP)] (eq 6). This result is not surprising considering the redox potential of **2** ($E_{½}$ = −1.34 V). After initial electron transfer, peaks corresponding to **1** diminish, with concomitant growth of features due to [Fe^{II}(NO)(TPP)] (1676 cm^{-1}) and **2** (1627, 1569 cm^{-1}). The appearance of **2** differs from the results for **1**, which revealed formation of **4** as a byproduct of NO-transfer (vide supra). In the reaction with an Fe(II) porphyrin, however, **1** must formally transfer an equivalent of NO· (not NO$^-$) to yield [Fe^{II}(NO)(TPP)]. Transfer of NO· from **1** generates an {Fe-NO}^{8} species (eq 7) that immediately disproportionates to give **2** (eq 8). Such a reaction sequence explains the observed IR spectral changes in Figure 9 with the net stoichiometry displayed in eq 9.

$$\underset{2,\left\{Fe(NO)_2\right\}^{10}}{\left[Fe(NO)_2\left(Ar-nacnac\right)\right]^-}+\left[Fe^{III}Cl\left(TPP\right)\right]\rightarrow\underset{1,\left\{Fe(NO)_2\right\}^{9}}{\left[Fe(NO)_2\left(Ar-nacnac\right)\right]}+\left[Fe^{II}\left(Cl\right)\left(TPP\right)\right]^- \quad (6)$$

$$\underset{1,\left\{Fe(NO)_2\right\}^{9}}{\left[Fe(NO)_2\left(Ar-nacnac\right)\right]}+\left[Fe^{II}Cl\left(TPP\right)\right]^-\rightarrow\underset{\{Fe-NO\}^{8}}{\left[Fe\left(NO\right)Cl\left(Ar-nacnac\right)\right]^-}+\underset{\{Fe-NO\}^{7}}{\left[Fe^{II}\left(NO\right)\left(TPP\right)\right]} \quad (7)$$

$$\underset{\{Fe-NO\}^{8}}{\left[Fe\left(NO\right)Cl\left(Ar-nacnac\right)\right]^-}\rightarrow 1/2\underset{2,\left[Fe(NO)_2\right]^{10}}{\left[Fe(NO)_2\left(Ar-nacnac\right)\right]^-}+1/2\left[Fe^{II}Cl_2\left(Ar-nacnac\right)\right]^- \quad (8)$$

$$\begin{aligned}&\underset{2,\left\{Fe(NO)_2\right\}^{10}}{\left[Fe(NO)_2\left(Ar-nacnac\right)\right]^-}\\&+\left[Fe^{III}Cl\left(TPP\right)\right]\rightarrow\underset{\{Fe-NO\}^{7}}{\left[Fe^{II}\left(NO\right)\left(TPP\right)\right]}\\&+1/2\underset{2,\left\{Fe(NO)_2\right\}^{10}}{\left[Fe(NO)_2\left(Ar-nacnac\right)\right]^-}\\&+1/2\left[Fe^{II}Cl_2\left(Ar-nacnac\right)\right]^-\end{aligned} \quad (9)$$

NO-transfer from **1** to independently prepared [Fe^{II}(TPP)] did not occur under the reactions conditions employed above for **2** and [Fe^{III}(TPP)Cl] (eqs 7 - 8). When Bu_4NCl was added to the reaction mixture, however, NO transfer proceeded as before over 4 h at ambient temperature. This result suggests that chloride may facilitate transfer of NO· from **1** to [Fe^{II}(TPP)]. The role of chloride is not yet known and kinetic experiments employing **2** and [Fe(TPP)Cl] could not be followed by UV-vis spectroscopy because the reaction proceeded too sluggishly at the concentrations required for optical spectroscopy, ~ 5 – 10 μM in porphyrin. This fact suggests that, unlike the reaction of **1** with [Fe^{III}(TPP)Cl], the rate-

limiting step for reaction of **1** with [Fe^{II}(TPP)] and Cl^- is overall bimolecular. Whether the reaction also depends on the concentration of Cl^- or [Fe^{II}(TPP)] is unknown at this time. A transition state or intermediate involving a chloride bridge is an attractive hypothesis, given the possibility for the DNIC/MNIC to adopt a five-coordinate geometry (vide supra, compound **4′**).

DISCUSSION

The transfer of NO ligands from dinitrosyl iron complexes to various acceptors has been demonstrated previously with several synthetic DNICs.[15,16,61] In many of these systems, the form of NO (NO·, NO^+ or NO^-) formally being transferred from the DNIC to the acceptor is dictated by the stability of the resulting nitrosylated or nitrosated product. Such dependence was noted previously in a study of NO-transfer from a cobalt nitrosyl to a variety of different metal complexes.[63] The reactivity suggests that NO-transfer reactions are dictated by the thermodynamic requirements of the acceptor and that different forms of NO may be released or transferred from the DNIC depending on the nature of the acceptor. Biologically, this characteristic of DNICs may be important, because the NO-acceptor may require NO· (heme sites), NO^- (oxidized heme sites), or NO^+ (thiols, amines, alcohols).

In the present work, we demonstrate a net formal transfer of both NO^-, $\{Fe(NO)_2\}^9$ to (TPP)Fe^{III}Cl, and of NO·, $\{Fe(NO)_2\}^9$ to (TPP)Fe^{II}. In each case the mechanism is distinct and the qualitative reaction rates under similar conditions are quite different. Formal transfer of NO^- from **1** to (TPP)Fe^{III}Cl operates as a unimolecular process with rate-limiting loss of NO· or NO^-. This mechanism is consistent with the observation that light irradiation increases the NO-transfer rate, because excitation of electrons to M–N antibonding orbitals should accelerate loss of a nitrosyl or nitroxyl ligand. In contrast, transfer of NO· from **1** to [Fe^{II}(TPP)] appears to be a bimolecular process. Furthermore, transfer of NO· does not occur in the absence of Cl^-. This fact suggests that coordination of a Lewis base to the DNIC may be required for the transfer of NO·, or perhaps that ligands capable of bridging two metal centers are important in mediating transfer of NO· between a DNIC and its metal targets.

In addition to NO-transfer reactions between DNICs and porphyrins, the related chemistry of MNICs was examined in the present work and deserves comment. Both four-coordinate $\{Fe\text{-}NO\}^7$ and $\{Fe\text{-}NO\}^8$ compounds disproportionate, forming DNICs and Fe(III) ($\{Fe\text{-}NO\}^7$) or Fe(II) ($\{Fe\text{-}NO\}^8$) compounds. In the case of the former, $\{Fe\text{-}NO\}^7$ compound, this reaction appears to be reversible judging by the fact that DNIC **1** and [$Fe^{III}Br_2$(Ar-nacnac)] (**6**) comproportionate in solution at 25 °C. Similar reactivity also occurs with four-coordinate MNICs containing thiolate ligands. These species also disprortionate, leading to DNICs and Fe(III) thiolates.[19] Such reactivity contrasts with that of five- and six-coordinate MNICs, which are stable with respect to disproportionation.

Reduction of **4** to give the unstable $\{Fe\text{-}NO\}^8$ species is intriguing, given its possible relevance to the mechanism of NO-scavenging reductases (sNORs).[64] These enzymes contain adjacent carboxylate-bridged $\{Fe\text{-}NO\}^7$ centers in their NO-bound state. In one proposed mechanism, reduction of both iron centers leads to formation of the corresponding

{Fe-NO}^{8} species. These reduced nitrosyls then revert back to diiron(II) species in the presence of protons with concomitant release of N_2O and H_2O. In the case of compound **4**, reduction to the {Fe-NO}^{8} leads to formation of a DNIC and *not* to chemistry at the NO ligands. The fact that Fe(II) is generated in the process, however, lends credence to the proposal that sNOR activity occurs through the intermediacy of an {Fe-NO}^{8} species.[65,66]

CONCLUSIONS

The NO-transfer chemistry of two dinitrosyl iron complexes supported by a sterically demanding β-diketiminate ligand has been explored using iron porphyrins as NO acceptors. The {Fe(NO)$_2$}^{9} DNIC, **1**, is capable of reductively nitrosylating [Fe^{III}(TPP)Cl)] at elevated temperatures or in the presence of light to afford [Fe^{II}(NO)(TPP)] and the corresponding {Fe-NO}^{7} complex, **4**. Preliminary kinetic measurements of this reaction point to a rate-limiting step involving dissociation of NO· or NO$^-$ from **1**. The analogous reaction of the {Fe(NO)$_2$}^{10} DNIC, **2**, also affords [Fe^{II}(NO)(TPP)], but in this instance rapid electron transfer from **2** to [Fe^{III}(TPP)Cl] precedes NO transfer. The resulting {Fe(NO)$_2$}^{9} DNIC then nitrosylates the Fe(II) porphyrin generating a {Fe-NO}^{8} species that immediately disproportionates to **2** and an NO-free Fe(II) complex, **5**. This chemistry was verified by the synthesis of MNIC **4** and examination of its redox chemistry. In addition to iron, a four-coordinate {Co(NO)$_2$}^{10} species, **3**, was isolated and fully characterized. The structural and spectroscopic properties of **3** are similar to those of the iron analogs, **1** and **2**. Compound **3** undergoes a quasi-reversible one-electron reduction to the putative {Co(NO)$_2$}^{11} species.

EXPERIMENTAL

General Comments

Manipulations of air- and moisture-sensitive materials were performed under an atmosphere of nitrogen gas using standard Schlenk techniques or in an MBraun glovebox under an atmosphere of purified nitrogen. Tetrahydrofuran, diethyl ether, pentane, benzene, and toluene were purified by passage through activated alumina[67] then stored over 4-Å molecular sieves prior to use. Benzene-d_6 and tetrahydrofuran-d_8 were dried over sodium ketyl and vacuum-distilled prior to use.

Materials

Compounds **1** and **2**,[45] (M)[Fe(NO)Br$_3$],[55] [Fe^{II}(TPP)],[68] [Co(μ-Cl)(NO)$_2$]$_2$,[53] KC_8, anhydrous Fe^{II}Br$_2$, and Cp*$_2$Co were synthesized according to published procedures. Na(Ar-nacnac)·2THF was prepared by deprotonation of H(Ar-nacnac) with NaN(SiMe$_3$)$_2$ in THF followed by crystallization from pentane. Li(Ar-nacnac) was prepared by deprotonation of H(Ar-nacnac) with ^{n}BuLi followed by crystallization from pentane at −30 °C. [Fe^{III}(TPP)Cl] and anhydrous Fe^{III}Br$_3$ were purchased from Strem Chemicals and used as received. Nitric oxide (Matheson, 99%) was purified by passage through an Ascarite column (NaOH fused on silica gel) and a 6-ft coil filled with silica gel cooled to −78 °C.[69] Purified NO gas was stored and transferred under an inert atmosphere using standard gas storage bulbs and gas-tight syringes, respectively. For NO-transfer reactions, care was taken

to prevent light exposure by covering reaction glassware in aluminum foil or by performing experiments in a darkened glovebox.

Physical Measurements

^{1}H NMR spectra were recorded on a Varian INOVA spectrometer operating at 500 MHz. FT-IR spectra were recorded with a ThermoNicolet Avatar 360 spectrophotometer running the OMNIC software; solid samples were pressed into KBr disks and solution samples were prepared in THF or benzene-d_6 in an air-tight Graseby-Specac solution cell with CaF_2 windows and 0.1 mm spacers. UV-vis spectra were recorded on a Cary-50 spectrophotometer in air-tight Teflon-capped quartz cells. Samples for ^{57}Fe Mössbauer studies were prepared by grinding solids with Apiezon-N grease. Samples were placed in a 90 K cryostat during measurement. All isomer shift (δ) and quadrupole splitting (ΔE_Q) values are reported with respect to ^{57}Fe-enriched metallic iron foil that was used for velocity calibration. The displayed spectrum was folded to enhance the signal-to-noise ratio. Fits of the data were calculated by the WMOSS version 2.5 plot and fit program.[70] X-band EPR spectra were recorded on a Bruker EMX EPR spectrometer. Temperature control was maintained with a quartz finger dewar (77 K). Spectra were recorded in 4 mm o.d. quartz EPR tubes capped with a tight-fitting rubber septum. Electrochemical measurements were performed at 25 °C on a VersaSTAT3 Princeton Applied Research potentiostat running the V3-Studio electrochemical analysis software. A 3-electrode set-up was employed comprising a glassy carbon working electrode, platinum wire auxiliary electrode, and a 0.1 M Ag/Ag^+ reference electrode. Triply recrystallized Bu_4NPF_6 or $Bu_4NBAr^F{}_4$ (Ar^F = 3,5-bis(trifluoromethyl)phenyl) was used as the supporting electrolyte. All electrochemical data were referenced internally to the ferrocene/ferrocenium couple at 0.00 V. Elemental analyses were performed by Midwest Microlab, LLC, Indianapolis, IN.

X-ray Data Collection and Structure Solution Refinement

Crystals of **3** - **6** suitable for X-ray diffraction were mounted in Paratone N oil using 30 μm aperture MiTeGen MicroMounts (Ithaca, NY) and frozen under a nitrogen cold stream maintained by a KRYO-FLEX low-temperature apparatus. Data were collected on a Bruker SMART APEX CCD X-ray diffractometer with Mo Kα radiation (λ = 0.71073 Å) controlled by the APEX2 software package (v. 2010.1-2). Data reduction was performed with SAINT.[71] Empirical absorption corrections were applied with SADABS,[72] and the structure was checked for higher symmetry by the PLATON software.[73] The structures were solved by direct methods with refinement by full-matrix least-squares based on F^2 using SHELXTL-97.[74] All non-hydrogen atoms were located and their positions refined anisotropically. Hydrogen atoms were assigned to idealized positions and given thermal parameters equal to either 1.5 (methyl hydrogen atoms) or 1.2 (non-methyl hydrogen atoms) times the thermal parameters of the atoms to which they were attached.

Crystals of **3** - **6** were grown by slow cooling of a saturated solution of each complex in pentane. No solvent was incorporated in any of the crystal lattices. The asymmetric unit of complex **3** contains two independent molecules with the same molecular structure. Complex **4** was modeled with a positional disorder between the NO and Br ligands. The N, O and Br atoms were located in the difference Fourier map and refined with 100% occupancy in each

of the two disordered components. See Table 1 for crystallographic data and additional refinement details.

[Co(NO)$_2$(Ar-nacnac)], 3

To 0.200 g (0.650 mmol) of [Co(μ-Cl)(NO)$_2$]$_2$ in 5 mL Et$_2$O was added a solution of 0.555 g (1.30 mmol) of Na(Ar-nacnac)·2THF in 10 mL Et$_2$O. The resulting brown-yellow solution was allowed to stir at ambient temperature for 2 h. All volatiles were removed in vacuo and the resulting residue was extracted into 10 mL of pentane. After filtration through a plug of Celite, the pentane solution was concentrated in vacuo to 3 mL and allowed to stand at −30 °C for 24 h. Compound **5** precipitated as 0.527 g (0.75%) of brown cubes in two crops. ^{1}H NMR (benzene-d_6): δ 7.07 (m, 6 ArH), 5.15 (s, 1 CH), 3.16 (sep, 4 CHMe$_2$), 1.73 (s, 6 Me), 1.23 (d, 12 CHMe$_2$), 1.15 (d, 12 CHMe$_2$). IR (benzene-d_6, cm^{-1}): 3057, 2963, 2928, 2869, 1801 (ν_{NO}), 1706 (ν_{NO}), 1554, 1522, 1458, 1438, 1399, 1316, 1177. CV (THF): $E_{½}$ = −1.80 V {Co(NO)$_2$}$^{10/11}$; E_{ox} = +0.53 V. UV-vis (THF) λ_{max}, nm (ε, M^{-1}cm^{-1}): 322 (6700), 360 (5700), 415 (sh), 570 (sh). Anal. Calcd for $C_{29}H_{41}CoN_4O_2$: C, 64.91; H, 7.70; N, 10.44. Found: C, 64.09; H, 7.58; N, 10.17.

[Fe(NO)Br(Ar-nacnac)], 4

Procedure A: To 0.114 g (0.250 mmol) of (Et$_4$N)[Fe(NO)Br$_3$] dissolved in 10 mL of THF was added a solution of 0.106 g (0.250 mmol) of Li(Ar-nacnac) in 5 mL THF. The solution immediately changed from yellow-brown to dark forest green upon addition of the diketiminate salt. The reaction was allowed to stir for an additional 2 h at ambient temperature, during which time the forest green solution changed to a dark brown mixture. All volatiles were removed in vacuo and the residue was extracted into 15 mL of pentane. The extract was filtered through a plug of Celite to remove Et$_4$NBr and LiCl. The resulting pentane solution was concentrated in vacuo to 5 mL and allowed to stand at −30 °C for 24 h. During this time compound **3** precipitated in two crops as 0.0886 g (61%) of brown cubes. See below for spectral data.

Procedure B: To 0.0530 g (0.099 mmol) of compound **4** in 2 mL THF was added 2.5 mL (~0.10 mmol) of NO gas via syringe. The solution immediately changed from bright yellow to dark brown. The solution was allowed to stir at ambient temperature for 20 min. All volatiles were removed in vacuo and the residue was extracted into 5 mL of pentane. After filtration through glass filter paper, the pentane solution was concentrated in vacuo to 2 mL and allowed to stand at −30 °C for 24 h. During this time, compound **3** precipitated as 0.0247 g (50%) of brown cubes; mp = 190 – 195 °C. ^{1}H NMR (benzene-d_6): δ 33.7 (2 H), 27.1 (2 H), 13.5 (v br, 1H), 4.5 (2 H), 3.7 (12 H), 2.8 (12 H), 1.4 (2 H), −21.2 (2 H), −33.2 (6 H). IR (benzene-d_6, cm^{-1}): 3060, 2965, 2927, 2869, 1777 (ν_{NO}), 1519, 1463, 1437, 1371, 1317, 1174, 1106, 1022; 1743 ($\nu_{^{15}NO}$). EPR (X-band, 2-MeTHF): 77 K g_1 = 4.62, g_2 = 3.41, g_3 = 1.96. CV (THF): $E_{½}$ = −1.23 V {Fe-NO}$^{7/8}$. UV-vis (THF) λ_{max}, nm (ε, M^{-1}cm^{-1}): 313 (19000), 417 (sh), 552 (1800). ^{57}Fe Mössbauer: δ = 0.33(2) mm/s, ΔE_Q = 0.92(2) mm/s, Γ = 0.44(2) mm/s. Anal. Calcd for $C_{29}H_{41}BrFeN_3O$: C, 59.70; H, 7.08; N, 7.20. Found: C, 60.19; H, 6.98; N, 7.41.

[Fe(THF)Br(Ar-nacnac)], 5

To 0.167 g (0.774 mmol) of anhydrous $Fe^{II}Br_2$ in 20 mL THF was added 0.454 g (0.776 mmol) of Na(Ar-nacnac)·2THF. The mixture was allowed to stir at ambient temperature for 2 h, during which time the color changed from orange to brown-yellow. The mixture was filtered through a plug of Celite to remove NaBr. All volatiles were removed in vacuo. The resulting residue was washed with pentane causing formation of a yellow precipitate. The solid was isolated by filtration and washed with pentane to give 0.377 g (85%) of **5** as a yellow powder. Storing the filtrate at −30 °C for 24 h afforded an additional 0.030 g of yellow needles that were used for X-ray diffraction. ^{1}H NMR (THF-d_8): δ 19.0, 7.0, 5.1, 1.1, 0.8, −8.8, −38.9, −68.9, −80.2. UV-vis (THF) λ_{max}, nm (ε, $M^{-1}cm^{-1}$): 331 (4200), 428 (sh); (toluene): 325 (11500), 389 (3500), 520 (670). CV (THF): $E_{½}$ = −0.61 V. Anal. Calcd for $C_{33}H_{49}BrFeN_2O$: C, 63.37; H, 7.90; N, 4.48. Found: C, 63.31; H, 7.68; N, 4.51.

[$Fe^{III}Br_2$(Ar-nacnac)], 6

This compound could only be prepared in small quantities by reaction of equimolar amounts of Na(Ar-nacnac)·2THF and anhydrous $FeBr_3$ in toluene. After stirring for 2 h at ambient temperature, all volatiles were removed in vacuo affording a dark forest green residue. Extraction of this residue into pentane generated a dark green solution and a large quantity of brown insoluble material, Fe(II) byproducts formed by reduction of Fe(III) by the diketiminate salt. The pentane solution was filtered through a plug of Celite, concentrated in vacuo, and allowed to stand at −35 °C for 24 h. After this time, small green cubes of **6** appeared (typically < 10 mg). These cubes were suitable for X-ray diffraction, but repeated elemental analysis and solution magnetic susceptibility measurements indicated that **6** contained diamagnetic impurities, most likely the coupled Ar-nacnac ligand. EPR (X-band, 2-MeTHF): 77 K g = 9.02, 5.24, 3.55, 2.60, 2.04, 1.30 (see SI). CV (THF): $E_{½}$ = −0.61 V.

General Procedure for NO-Transfer Reactions

Solutions of **1** or **2** in THF (UV-vis) or benzene-d_6 (IR) were prepared in the glovebox at appropriate concentrations (~100 μM for UV, ~20 mM for IR). These solutions were then combined with a solution of the desired iron porphyrin compound in a vial or quartz cuvette. Reactions were allowed to proceed in the absence of light as much as possible. For UV-vis reactions conducted in the presence of light irradiation, the cuvette was exposed to fluorescent room light for 3 min intervals between spectra.

Supplementary Material

Refer to Web version on PubMed Central for supplementary material.

Acknowledgements

This work was supported by grant CHE-0907905 from the National Science Foundation. Z.J.T. acknowledges NIGMS for a postdoctoral fellowship, F32 GM082031-03.

REFERENCES

(1). Vanin AF. Nitric Oxide. 2009; 21:1–13. [PubMed: 19366636]

(2). Alencar JL, Chalupsky K, Sarr M, Schini-Kerth V, Vanin AF, Stoclet J-C, Muller B. Biochem. Pharmacol. 2003; 66:2365–2374. [PubMed: 14637194]

(3). Vanin AF. Biochemistry (Moscow). 1998; 63:782–793. [PubMed: 9721330]

(4). Vanin AF, Stukan RA, Manukhina EB. Biochim. Biophys. Acta, Protein Struct. Mol. Enzymol. 1996; 1295:5–12.

(5). Boese M, Mordvintcev PI, Vanin AF, Busse R, Mülsch A. J. Biol. Chem. 1995; 270:29244–29249. [PubMed: 7493954]

(6). Chen Y-J, Ku W-C, Feng L-T, Tsai M-L, Hsieh C-H, Hsu W-H, Liaw W-F, Hung C-H, Chen Y-J. J. Am. Chem. Soc. 2008; 130:10929–10938. [PubMed: 18661983]

(7). Mokh VP, Poltorakov AP, Serezhenkov VA, Vanin AF. Nitric Oxide. 2010; 22:266–274. [PubMed: 20067839]

(8). Bosworth CA, Toledo JC Jr. Zmijewski JW, Li Q, Lancaster JR Jr. Proc. Natl. Acad. Sci. U.S.A. 2009; 106:4671–4676. [PubMed: 19261856]

(9). Chang H-H, Huang H-J, Ho Y-L, Wen Y-D, Huang W-N, Chiou S-J. Dalton Trans. 2009:6396–6402. [PubMed: 19655074]

(10). Wecksler SR, Hutchinson J, Ford PC. Inorg. Chem. 2006; 45:1192–1200. [PubMed: 16441130]

(11). Wen Y-D, Ho Y-L, Shiau R-J, Yeh J-K, Wu J-Y, Wang W-L, Chiou S-J. J. Organomet. Chem. 2010; 695:352–359.

(12). Sanina NA, Roudneva TN, Shilov GV, Morgunov R, Ovanesyan NS, Aldoshin SM. Dalton Trans. 2009:1703–1706. [PubMed: 19240901]

(13). Ostrowski AD, Ford PC. Dalton Trans. 2009:10660–10669. [PubMed: 20023893]

(14). Dillinger SAT, Schmalle HW, Fox T, Berke H. Dalton Trans. 2007:3562–3571. [PubMed: 17680047]

(15). Lu T-T, Chen C-H, Liaw W-F. Chem.-Eur. J. 2010; 16:8088–8095. [PubMed: 20533462]

(16). Chiang C-Y, Darensbourg M. J. Biol. Inorg. Chem. 2006; 11:359–370. [PubMed: 16520978]

(17). Ueno T, Suzuki Y, Fujii S, Vanin AF, Yoshimura T. Biochem. Pharmacol. 2002; 63:485–493. [PubMed: 11853699]

(18). Hsieh C-H, Darensbourg MY. J. Am. Chem. Soc. 2010; 132:14118–14125. [PubMed: 20857969]

(19). Butler AR, Glidewell C, Li M-H. Adv. Inorg. Chem. 1988; 32:335–393.

(20). Butler AR, Megson IL. Chem. Rev. 2002; 102:1155–1165. [PubMed: 11942790]

(21). Chiang CY, Miller ML, Reibenspies JH, Darensbourg MY. J. Am. Chem. Soc. 2004; 126:10867–10874. [PubMed: 15339171]

(22). Cesareo E, Parker LJ, Pedersen JZ, Nuccetelli M, Mazzetti AP, Pastore A, Federici G, Caccuri AM, Ricci G, Adams JJ, Parker MW, Bello ML. J. Biol. Chem. 2005; 280:42172–42180. [PubMed: 16195232]

(23). Lee M, Arosio P, Cozzi A, Chasteen ND. Biochemistry. 1994; 33:3679–3687. [PubMed: 8142366]

(24). Toledo JC Jr. Bosworth CA, Hennon SW, Mahtani HA, Bergonia HA, Lancaster JR Jr. J. Biol. Chem. 2008; 283:28926–28933. [PubMed: 18480062]

(25). Ren B, Duan X, Ding H. J. Biol. Chem. 2009; 284:4829–4835. [PubMed: 19074432]

(26). Duan X, Yang J, Ren B, Tan G, Ding H. Biochem. J. 2009; 417:783–789. [PubMed: 18945212]

(27). Ren B, Zhang N, Yang J, Ding H. Mol. Microbiol. 2008; 70:953–964. [PubMed: 18811727]

(28). Rogers PA, Eide L, Klungland A, Ding H. DNA Repair. 2003; 2:809–817. [PubMed: 12826281]

(29). Foster MW, Cowan JA. J. Am. Chem. Soc. 1999; 121:4093–4100.

(30). Sellers VM, Johnson MK, Dailey HA. Biochemistry. 1996; 35:2699–2704. [PubMed: 8611576]

(31). Reddy D, Lancaster JR Jr. Cornforth DP. Science. 1983; 221:769–770. [PubMed: 6308761]

(32). Enemark JH, Feltham RD. Coord. Chem. Rev. 1974; 13:339–406.

(33). Vanin AF, Serezhenkov VA, Mikoyan VD, Genkin MV. Nitric Oxide. 1998; 2:224–234. [PubMed: 9851363]

(34). Ye S, Neese F. J. Am. Chem. Soc. 2010; 132:3646–3647. [PubMed: 20196538]

(35). Tsai M-C, Tsai F-T, Lu T-T, Tsai M-L, Wei Y-C, Hsu I-J, Lee J-F, Liaw W-F. Inorg. Chem. 2009; 48:9579–9591. [PubMed: 19746902]
(36). Hopmann KH, Conradie J, Ghosh A. J. Phys. Chem. B. 2009; 113:10540–10547. [PubMed: 19719290]
(37). Conradie J, Quarless DA, Hsu HF, Harrop TC, Lippard SJ, Koch SA, Ghosh A. J. Am. Chem. Soc. 2007; 129:10446–10456. [PubMed: 17685516]
(38). Tsai F-T, Chiou S-J, Tsai M-C, Tsai M-L, Huang H-W, Chiang M-H, Liaw W-F. Inorg. Chem. 2005; 44:5872–5881. [PubMed: 16060642]
(39). Bryar TR, Eaton DR. Can. J. Chem. 1992; 70:1917–1926.
(40). Mutus, B. Nitric Oxide Donors. Wang, PG.; Cai, TB.; Taniguchi, N., editors. WILEY-VCH Verlag GmbH & Co KGaA; Weinheim: 2005. p. 91-109.
(41). Ng ESM, Kubes P. Can. J. Physiol. Pharmacol. 2003; 81:759–764. [PubMed: 12897804]
(42). Atkinson FL, Blackwell HE, Brown NC, Connelly NG, Crossley JG, Orpen AG, Rieger AL, Rieger PH. J. Chem. Soc., Dalton Trans. 1996:3491–3502.
(43). Lu T-T, Tsou C-C, Huang H-W, Hsu I-J, Chen J-M, Kuo T-S, Wang Y, Liaw W-F. Inorg. Chem. 2008; 47:6040–6050. [PubMed: 18517190]
(44). Tsou C-C, Lu T-T, Liaw W-F. J. Am. Chem. Soc. 2007; 129:12626–12627. [PubMed: 17900121]
(45). Tonzetich ZJ, Do LH, Lippard SJ. J. Am. Chem. Soc. 2009; 131:7964–7965. [PubMed: 19459625]
(46). Holland PL. Acc. Chem. Res. 2008; 41:905–914. [PubMed: 18646779]
(47). Puiu SC, Warren TH. Organometallics. 2003; 22:3974–3976.
(48). Wang X, Sundberg EB, Li L, Kantardjieff KA, Herron SR, Lim M, Ford PC. Chem. Commun. 2005:477–479.
(49). Reginato N, McCrory CTC, Pervitsky D, Li L. J. Am. Chem. Soc. 1999; 121:10217–10218.
(50). Tsai M-L, Liaw W-F. Inorg. Chem. 2006; 45:6583–6585. [PubMed: 16903707]
(51). Haymore B, Feltham RD. Inorg. Synth. 1973; 14:81–89.
(52). Tennyson AG, Dhar S, Lippard SJ. J. Am. Chem. Soc. 2008; 130:15087–15098. [PubMed: 18928257]
(53). Sacco A, Rossi M, Nobile CF. Ann. Chim. (Rome). 1967; 57:499–507.
(54). Harrop TC, Song D, Lippard SJ. J. Am. Chem. Soc. 2006; 128:3528–3529. [PubMed: 16536520]
(55). Connelly NG, Gardner C. J. Chem. Soc., Dalton Trans. 1976:1525–1527.
(56). Lu T-T, Chiou S-J, Chen C-Y, Liaw W-F. Inorg. Chem. 2006; 45:8799–8806. [PubMed: 17029392]
(57). Hauser C, Glaser T, Bill E, Weyhermuller T, Wieghardt K. J. Am. Chem. Soc. 2000; 122:4352–4365.
(58). Eckert NA, Smith JM, Lachicotte RJ, Holland PL. Inorg. Chem. 2004; 43:3306–3321. [PubMed: 15132641]
(59). Panda A, Stender M, Wright RJ, Olmstead MM, Klavins P, Power PP. Inorg. Chem. 2002; 41:3909–3916. [PubMed: 12132915]
(60). Shimokawa C, Itoh S. Inorg. Chem. 2005; 44:3010–3012. [PubMed: 15847404]
(61). Harrop TC, Song D, Lippard SJ. J. Inorg. Biochem. 2007; 101:1730–1738. [PubMed: 17618690]
(62). Scheidt WR, Ellison MK. Acc. Chem. Res. 1999; 32:350–359.
(63). Ungermann CB, Caulton KG. J. Am. Chem. Soc. 1976; 98:3862–3868.
(64). Kurtz DM. Dalton Trans. 2007:4115–4121.
(65). Hayashi T, Caranto JD, Wampler DA, Kurtz DM, Moënne-Loccoz P. Biochemistry. 2010; 49:7040–7049. [PubMed: 20669924]
(66). Silaghi-Dumitrescu R, Ng KY, Viswanathan R, Kurtz DM. Biochemistry. 2005; 44:3572–3579. [PubMed: 15736966]
(67). Pangborn AB, Giardello MA, Grubbs RH, Rosen RK, Timmers FJ. Organometallics. 1996; 15:1518–1520.
(68). Hu C, Noll BC, Schulz CE, Scheidt WR. Inorg. Chem. 2007; 46:619–621. [PubMed: 17257003]

(69). Lim, MD.; Lorković, IM.; Ford, PC. Methods Enzymol. Vol. 396. Academic Press; 2005. p. 3-17.

(70). Kent, TA. *WMOSS* v. 2.5: Mössbauer Spectral Analysis Software. WEB Research Co.; Minneapolis, MN: 1998.

(71). Sheldrick GM. Acta Crystallogr., Sect. A. 2008; A64:112–122. [PubMed: 18156677]

(72). Sheldrick, GM. *SADABS*: Area-Detector Absorption Correction. University of Göttingen; Göttingen, Germany: 2001.

(73). Spek, AL. *PLATON*, A Multipurpose Crystallographic Tool. Utrecht University; Utrecht, The Netherlands: 2000.

(74). Sheldrick, GM. *SHELXTL97*: Program for Refinement of Crystal Structures. University of Göttingen; Göttingen, Germany: 1997.

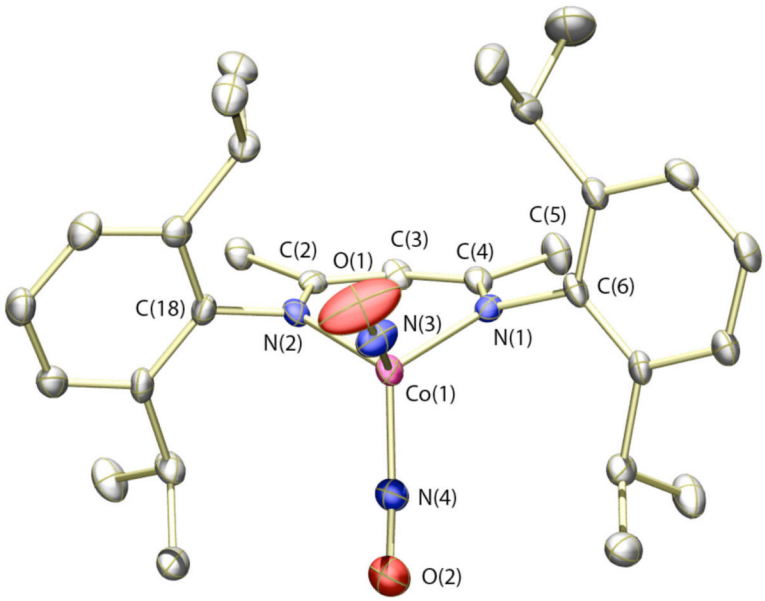

Figure 1.

Thermal ellipsoid (50%) rendering of one of the two crystallographically independent molecules of **3** in the asymmetric unit. Hydrogen atoms omitted for clarity. Selected bond distances (Å) and angles (deg): Co(1)–N(1) = 1.955(4); Co(1)–N(2) = 1.957(4); Co(1)–N(3) = 1.633(3); Co(1)–N(4) = 1.695(4); N(3)–O(1) = 1.165(5); N(4)–O(2) = 1.166(5); Co(1)–N(3)–O(1) = 173.0(4); Co(1)–N(4)–O(2) = 150.1(4); N(3)–Co(1)–N(4) = 110.5(2).

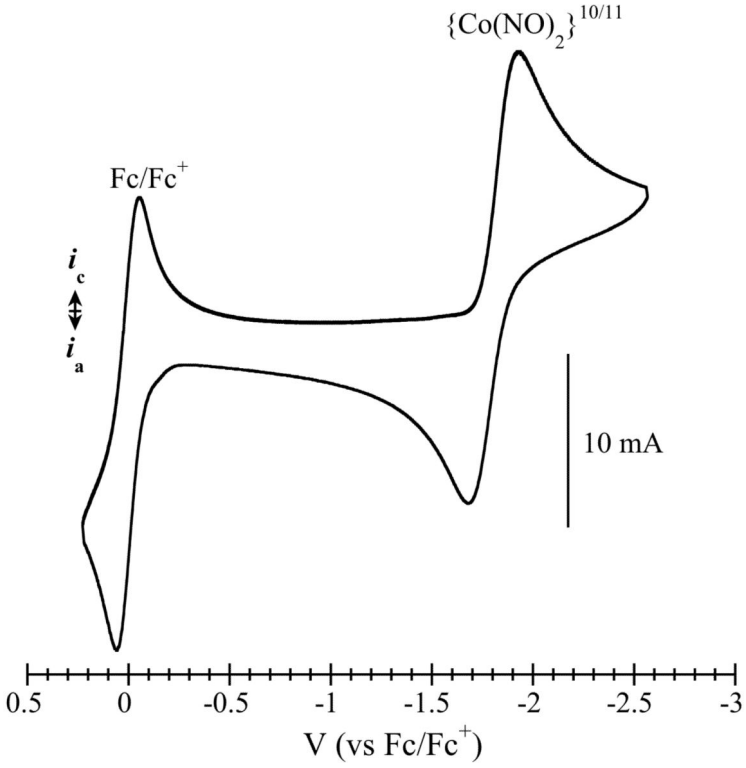

Figure 2.

Cyclic voltammogram of compound **3** in tetrahydrofuran at a glassy carbon electrode (0.1 M $Bu_4BAr^F{}_4$ supporting electrolyte; 50 mV/s scan rate). Fc/Fc^+ indicates the ferrocene reference couple.

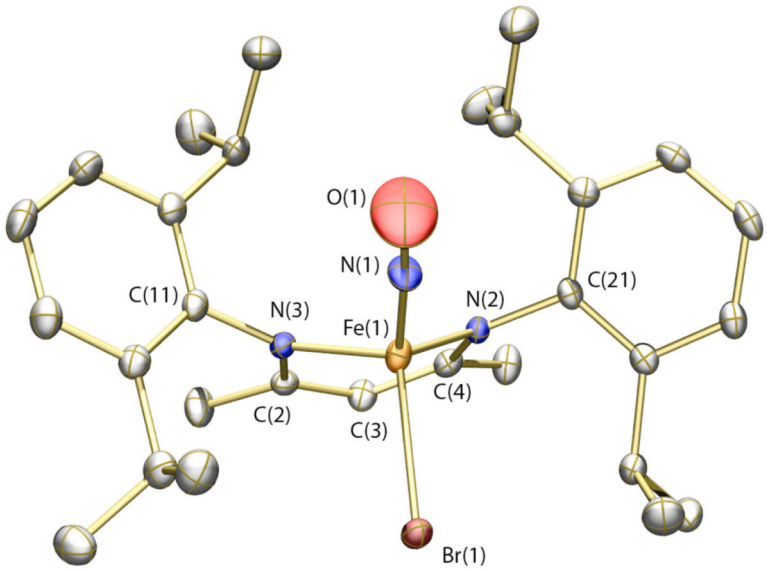

Figure 3.

Thermal ellipsoid (50%) rendering of the solid-state structure of **4**. The major component of the disordered structure is pictured. Hydrogen atoms are omitted for clarity. Selected bond distances (Å) and angles (deg): Fe(1)–N(1) = 1.644(5); Fe(1)–N(2) = 1.971(2); Fe(1)–N(3) = 1.938(2); N(1)–O(1) 1.217(6); Fe(1)–Br(1) = 2.4136(9); O(1)–N(1)–Fe(1) = 175.5(6); N(1)–Fe(1)–Br(1) = 115.22(15).

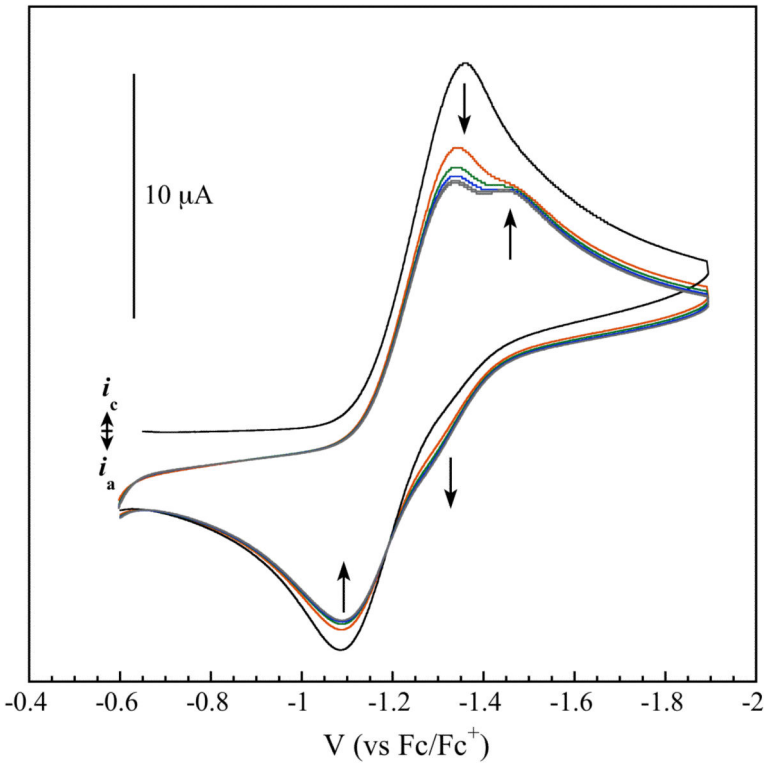

Figure 4.

Cyclic voltammogram (100 mV/s) of [Fe(NO)Br(Ar-nacnac)] indicating disproportionation of the $\{Fe\text{-}NO\}^8$ species to $\{Fe(NO)_2\}^{10}$ and "Fe(II)". The traces were recorded at a glassy carbon electrode in THF with 0.1 M Bu_4NPF_6 as supporting electrolyte.

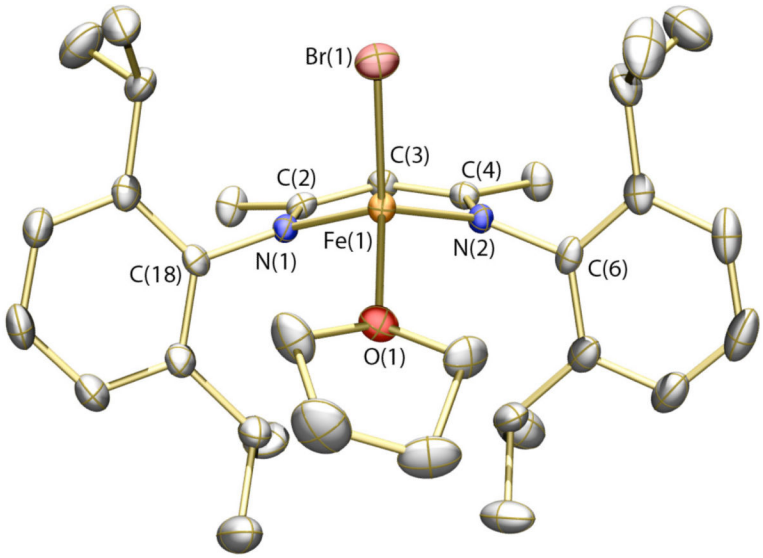

Figure 5.

Thermal ellipsoid (50%) rendering of the solid-state structure of **5**. Hydrogen atoms omitted for clarity. Selected bond distances (Å) and anlges (deg): Fe(1)–N(1) 2.010(3); Fe(1)–N(2) 1.999(3); Fe(1)–O(1) 2.062(3); Fe(1)–Br(1) 2.4114(6); Br(1)–Fe(1)–O(1) = 98.50(7).

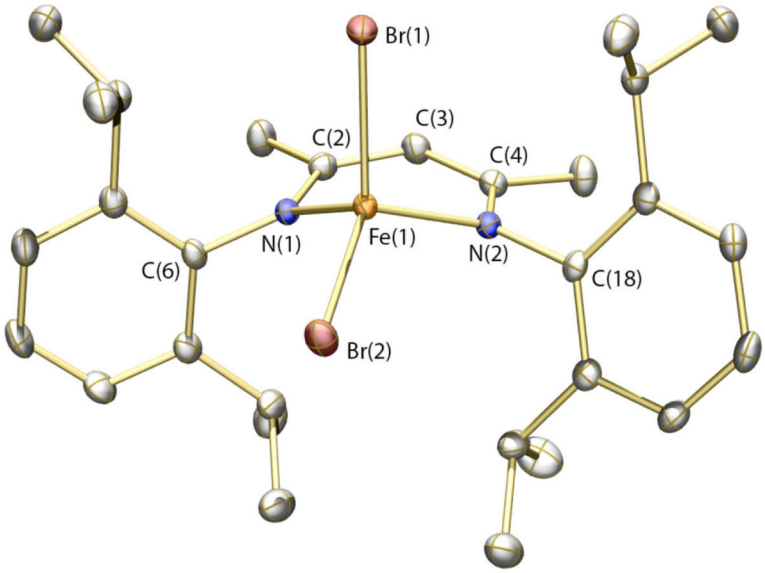

Figure 6.

Thermal ellipsoid (50%) rendering of the solid-state structure of **6**. Hydrogen atoms omitted for clarity. Selected bond distances (Å) and angles (deg): Fe(1)–N(1) = 1.9459(13); Fe(1)–N(2) = 1.9730(13); Fe(1)–Br(1) = 2.3446(3); Fe(1)–Br(2) = 2.3188(3); Br(1)–Fe(1)–Br(2) = 116.068(11).

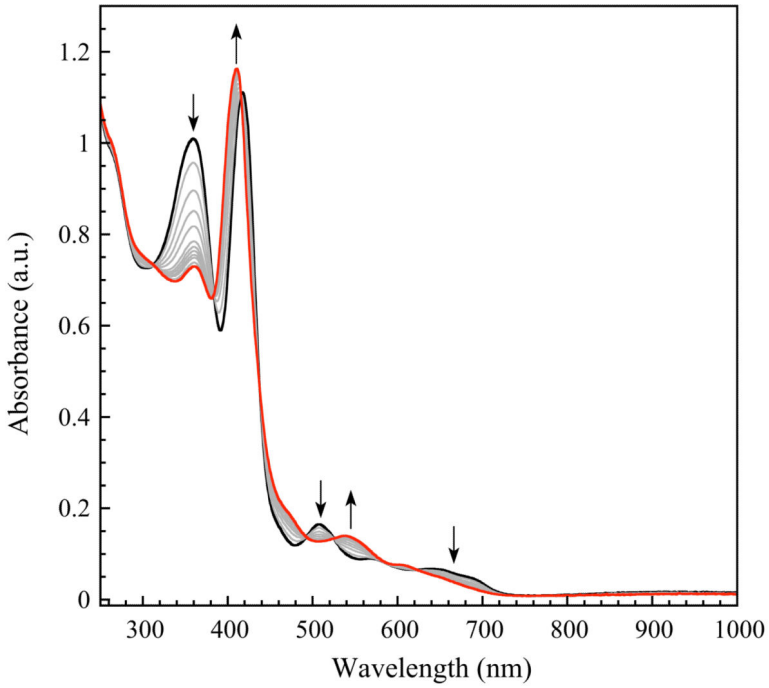

Figure 7.

UV-vis spectral changes associated with the reaction of $[Fe(NO)_2(Ar\text{-}nacnac)]$ with $[Fe^{III}(TPP)Cl]$ in tetrahydrofuran with exposure to ordinary room light.

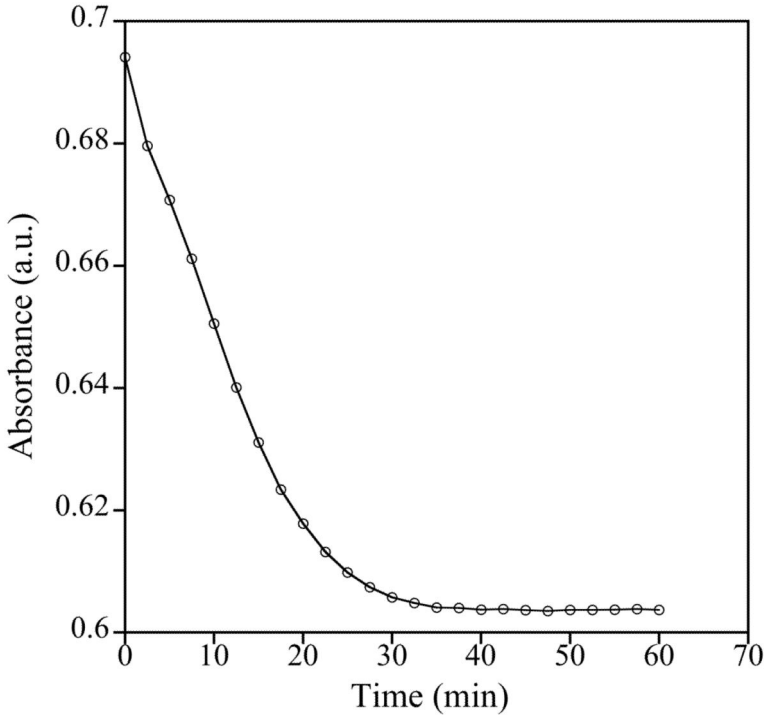

Figure 8.

Representative kinetic trace (single wavelength, 419 nm) for the reaction of 95 μM **1** with 4.7 μM [Fe^{III}(TPP)Cl] in toluene at 60 °C.

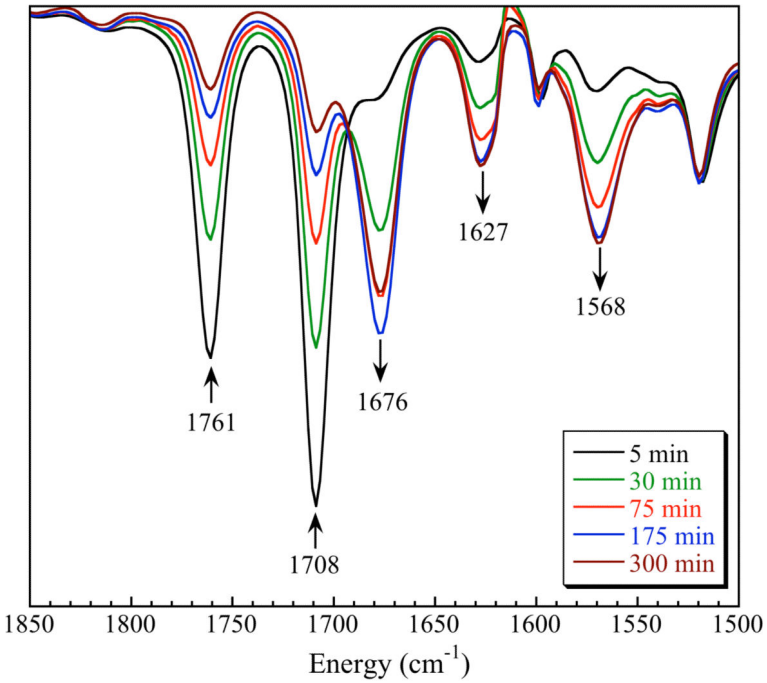

Figure 9.

IR spectral changes associated with the reaction of $(Bu_4N)[Fe(NO)_2(Ar\text{-}nacnac)]$ with [Fe(TPP)Cl] in C_6D_6 at 25 °C. The decrease in intensity of the peak at 1676 cm^{-1} after 300 min is due to precipitation of [Fe(NO)(TPP)].

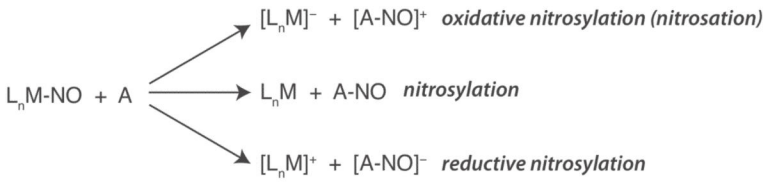

Scheme 1.

Different scenarios for transfer of NO between donor (L_nM) and acceptor (A).

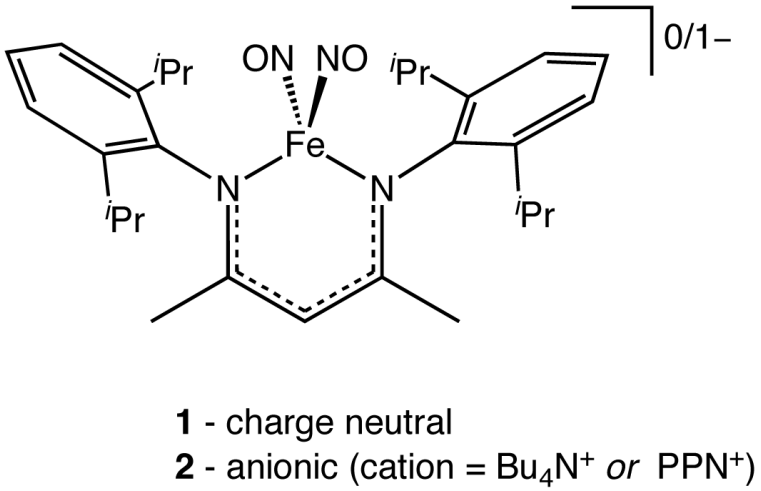

Chart 1.
Chemical structures of compounds **1** and **2**.

Table 1

X-ray Data Collection and Refinement Parameters for Compounds **3 - 6**

	3	**4**	**5**	**6**
Empirical formula	$C_{29}H_{41}CoN_4O_2$	$C_{29}H_{41}BrFeN_3O$	$C_{33}H_{49}BrFeN_2O$	$C_{29}H_{41}FeN_2Br_2$
Formula weight (g/mol)	536.59	583.41	625.50	633.31
Temperature (K)	100(2)	110(2)	110(2)	100(2)
Crystal system, space group	Triclinic, $P\bar{1}$	Monoclinic, $P2_1/n$	Monoclinic, $P2_1/n$	Monoclinic, $P2_1/n$
Unit cell dimensions	a = 12.590(2) Å b = 16.240(3) Å c = 16.649(3) Å α = 111.071(3)° β = 99.370(3)° γ = 109.899(3)°	a = 12.442(3) Å b = 20.007(5) Å c = 13.102(3) Å β = 115.805(4)°	a = 10.1792(6) Å b = 14.7884(8) Å c = 21.7305(13) Å β = 93.3570(10)°	a = 12.5714(10) Å b = 19.9181(16) Å c = 13.2247(11) Å β = 116.9340(10)°
Volume ($Å^3$)	2824.8(8)	2936.2(12)	3265.6(3)	2952.2(4)
Z, Calculated density (g/cm^3)	4, 1.262	4, 1.320	4, 1.272	4, 1.425
Absorption coefficient (mm^{-1})	0.639	1.899	1.711	3.237
F(000)	1144	1220	1320	1300
Crystal size (mm)	0.13 × 0.06 × 0.05	0.28 × 0.17 × 0.13	0.40 × 0.24 × 0.20	0.24 × 0.18 × 0.14
Θ range	1.39 to 24.71°	1.89 to 29.57°	1.67 to 25.03°	1.86 to 26.33°
Limiting indices	−14 ≤ *h* ≤ 14, −19 ≤ *k* ≤ 19, −19 ≤ *l* ≤ 19	−17 ≤ *h* ≤ 17, −27 ≤ *k* ≤ 27, −18 ≤ *l* ≤ 18	−12 ≤ *h* ≤ 12, −17 ≤ *k* ≤ 17, −25 ≤ *l* ≤ 25	−15 ≤ *h* ≤ 15, −24 ≤ *k* ≤ 24, −16 ≤ *l* ≤ 16
Reflections collected / unique	42216 / 9575 [R(int) = 0.1065]	64961 / 8235 [R(int) = 0.0628]	52989 / 5786 [R(int) = 0.0290]	52094 / 5987 [R(int) = 0.0302]
Completeness to Θ	99.5%	100%	99.9%	99.6%
Absorption correction	Empirical	Empirical	Empirical	Empirical
Max. and min. transmission	0.9688 and 0.9215	0.7904 and 0.6184	0.7259 and 0.5476	0.6600 and 0.5105
Data / restraints / parameters	9575 / 0 / 653	8235 / 62 / 354	5786 / 0 / 346	5987 / 0 / 317
Goodness-of-fit on F^2	1.018	1.294	1.265	1.043
Final R indices [I > 2σ(I)]	R1 = 0.0599, wR2 = 0.1235	R1 = 0.0554, wR2 = 0.1103	R1 = 0.0431, wR2 = 0.0992	R1 = 0.0203, wR2 = 0.0506
R indices (all data)	R1 = 0.1132, wR2 = 0.1465	R1 = 0.0691, wR2 = 0.1138	R1 = 0.0446, wR2 = 0.0999	R1 = 0.0236, wR2 = 0.0520
Largest diff. peak and hole ($e·Å^{-3}$)	0.852 and −0.524	0.466 and −0.523	0.936 and −0.574	0.609 and −0.292

Refinement method was full-matrix least-squares on F^2; wavelength = 0.71073 Å.

$R_1 = \Sigma||F_o|-|F_c||/\Sigma|F_o|$; $wR_2 = \{\Sigma[w(F_o^2-F_c^2)^2]/\Sigma[w(F_o^2)^2]\}^{1/2}$.